第 36 卷第 1 期 无 机 化 学 学 报 Vol.36 No.1
2020 年 1 月 CHINESE JOURNAL OF INORGANIC CHEMISTRY 173-182

基于芳香四羧酸构筑的两种配位聚合物的荧光及磁性质

翟丽军[1,2] 张 婕[1] 高玲玲[1] 高 婷[1] 贾焦焦[1,2] 牛宇岚*[,2] 胡拖平*[,1]
([1]中北大学理学院化学系,太原 030051)
([2]太原工业学院化学与化工系,太原 030008)

摘要:在溶剂热条件下,基于芳香四羧酸合成了 2 种新颖的配位聚合物:$\{[Zn_2(tptc)(1,4\text{-bimb})_2]\cdot H_2O\}_n$ (**1**)和$\{[Ni(tptc)_{0.5}(1,2\text{-bimb})(H_2O)]\cdot H_2O\}_n$ (**2**),其中,tptc 为对-三联苯-3,3″,5,5″-四羧酸,1,4-bimb 为 1,4-二(咪唑-1-亚甲基)苯,1,2-bimb 为 1,2-二(咪唑-1-亚甲基)苯。结构分析表明,**1** 为三维结构,拓扑符号为(8^6);**2** 为二维层状网络,通过氢键相互作用进一步扩展为三维超分子结构。此外,我们还研究了 **1** 对阳离子、阴离子的荧光感应以及 **2** 的磁性质。

关键词:芳香四羧酸;配位聚合物;荧光性质;磁性质
中图分类号:O614.24+1;O614.81+3 **文献标识码**:A **文章编号**:1001-4861(2020)01-0173-10
DOI:10.11862/CJIC.2019.257

Two Coordination Polymers Constructed by Aromatic Tetracarboxylic Acid: Luminescent and Magnetic Properties

ZHAI Li-Jun[1,2] ZHANG Jie[1] GAO Ling-Ling[1] GAO Ting[1]
JIA Jiao-Jiao[1,2] NIU Yu-Lan*[,2] HU Tuo-Ping*[,1]
([1]*Department of Chemistry, College of Science, North University of China, Taiyuan* 030051, *China*)
([2]*Department of Chemistry and Chemical Engineering, Taiyuan Institute of Technology, Taiyuan* 030008, *China*)

Abstract: Two new coordination polymers (CPs) based on H_4tptc, namely, $\{[Zn_2(tptc)(1,4\text{-bimb})_2]\cdot H_2O\}_n$ (**1**) and $\{[Ni(tptc)_{0.5}(1,2\text{-bimb})(H_2O)]\cdot H_2O\}_n$ (**2**) (H_4tptc=*p*-terphenyl-3,3″,5,5″-tetracarboxylic acid, 1,4-bimb=1,4-bis (imidazol-1-ylmethyl) benzene, 1,2-bimb=1,2-bis (imidazol-1-ylmethyl) benzene), have been synthesized under solvothermal conditions. The structural analyses reveal that complex **1** shows a 3D structure with the symbol of (8^6), while complex **2** presents a 2D layer network, which is further expanded into a 3D supramolecular structure through H-bonding interactions. Furthermore, the luminescence sensing of **1** for cations, anions as well as magnetic property of **2** have also been studied. CCDC: 1911100, **1**; 1911101, **2**.

Keywords: aromatic tetracarboxylic acid; coordination polymers; luminescent properties; magnetic properties

Coordination polymers (CPs) have caused extensive attention from researchers as a new kind of functional hybrid materials because they have fascinating structures and extensive application in gas storage and separation[1-4], optics properties[5-10], magnetism[11-12], catalysis[13-14] and drug sustained release[15], *etc*. At present, there have also been a lot of reports on the research of CPs in luminescence probe. Compared with traditional instrument methods, luminescence sensing is considered as a promising method due to its advantages of quick response, high sensitivity, low cost, simple operation, and so on[16-18].

收稿日期:2019-06-26。收修改稿日期:2019-10-01。
山西省国际科技合作项目(No.201803D421080)资助。
*通信联系人。E-mail:hutuoping@nuc.edu.cn,niuyulan@163.com

In the past few years, with the rapid development of economy and the explosive growth of the population, the problems such as environmental pollution and public health are arousing more and more concerns[19]. Fe^{3+} is not only necessary for metabolism, but also widely used in industry[20]. However, excessive amounts of Fe^{3+} in the human body are harmful, and Fe^{3+} can contaminate the environment by being carelessly discarded[21]. While Cr^{6+} is widely used in diverse industrial applications, improper disposal of Cr^{6+} will pollute the living conditions of people[22]. So, it is very urgent to synthesize materials that can selectively and sensitively identify these ions. In recent years, researchers have agreed that CPs are one of the promising alternatives for luminescent probe. One of the biggest challenges is the design and construction of CPs with stable structure and ideal function. In the process of self-assembly, the construction of the desired CPs depends on organic ligands and metal ions[23]. In terms of ligands, studies have shown that aromatic polycarboxylic acids are extensively used to construct CPs due to the following advantages: firstly, their multiple binding nodes; secondly, their carboxylate groups can be partially or completely deprotonated to form multiple structures; furthermore, aromatic conjugated systems can coordinate with d^{10} center ions forming CPs materials with excellent luminescence properties. At the same time, the introduction of the second nitrogen-containing ligand is helpful to construct CPs with novel structures.

So, based on the ligands of *p*-terphenyl-3,3″,5,5″-tetracarb oxylic acid (H_4tptc), 1,4-bis(imidazol-1-ylmethyl) benzene (1,4-bimb) or 1,2-bis(imidazol-1-ylmethyl) benzene (1,2-bimb) (Scheme 1), two novel CPs, namely $\{[Zn_2(tptc)(1,4\text{-bimb})_2]\cdot H_2O\}_n$ (**1**) and $\{[Ni(tptc)_{0.5}(1,2\text{-bimb})(H_2O)]\cdot H_2O\}_n$ (**2**), have been synthesized under solvothermal method and characterized by luminescence properties (**1**) and magnetic properties (**2**).

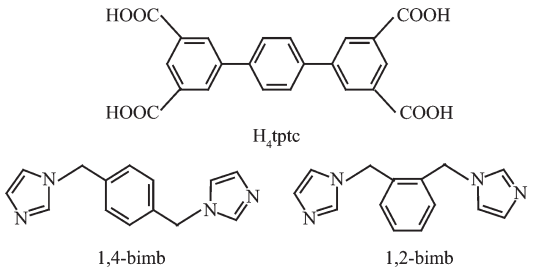

Scheme 1 Structures of the ligands

1 Experimental

1.1 Materials and physical measurements

All chemicals were purchased commercially and used without further purification. IR (KBr pellet) spectra were recorded under a FTIR-8400S spectrometer in a range of 4 000~400 cm^{-1}. Thermogravimetric analyses (TGA) were collected on a METTLER TGA analyzer at a heating rate of 10 ℃·min^{-1} under N_2 atmosphere from room temperature to 750 ℃. Elemental analyses (C, H, and N) were performed by using a PerkinElmer 2400C elemental analyzer (EA). Powder X-ray diffraction (PXRD) was performed using a Rigaku D/Max-2500 PC diffractometer (Mo $K\alpha$ radiation, λ=0.154 06 nm) at 50 kV, 30 mA with the 2θ range of 5°~50°. Luminescence spectra were performed on Hitachi F4600 spectrophotometer. Magnetic properties were measured by Quantum Design MPMS-XL-7 SQUID magnetometer.

1.2 Synthesis of the complexes

1.2.1 Synthesis of $\{[Zn_2(tptc)(1,4\text{-bimb})_2]\cdot H_2O\}_n$ (**1**)

$Zn(NO_3)_2\cdot 6H_2O$ (0.015 mmol, 4.5 mg), H_4tptc (0.005 mmol, 2.1 mg), 1,4-bimb (0.005 mmol, 1.2 mg), 0.15 mL NaOH aqueous solution (0.5 mol·L^{-1}) and 1 mL H_2O/DMF (1∶1, *V*/*V*) were mixed in a stainless steel vessel (25 mL), kept at 130 ℃ for 72 h and then naturally cooled to ambient temperature to obtain colorless crystals. Yield: 41% (based on Zn). Elemental analysis Calcd. for $C_{50}H_{40}N_8O_9Zn_2$(%): C, 58.48; H, 3.91; N, 10.85. Found(%): C, 58.54; H, 3.95; N, 10.89. IR (KBr, cm^{-1}): 3 455 (m), 1 630 (s), 1 524 (vs), 1 393 (s), 742 (s), 733 (s), 683 (m), 678 (m) (Supporting information, Fig.S1).

1.2.2 Synthesis of $\{[Ni(tptc)_{0.5}(1,2\text{-bimb})(H_2O)]\cdot H_2O\}_n$ (**2**)

$Ni(NO_3)_2\cdot 6H_2O$ (0.03 mmol, 8.8 mg), H_4tptc (0.01 mmol, 4.2 mg), 1,2-bimb (0.02 mmol, 4.8 mg) and 8 mL CH_3CN/H_2O (1∶1, *V*/*V*) were placed in a 25 mL autoclave and heated to 130 ℃ for 72 h. After slowly

being cooled to ambient temperature, green crystals were gained. Yield: 46% (based on Ni). Elemental Analysis Calcd. for $C_{25}H_{23}N_4NiO_6$ (%): C, 56.16; H, 4.30; N, 10.48. Found(%): C, 56.24; H, 4.25; N, 10.68. IR (KBr, cm^{-1}): 3 402 (vs), 1 613 (vs), 1 546 (vs), 1 526 (s), 1 402 (vs), 1 371 (s), 986 (m), 977 (m). 870 (s), 782 (s), 773 (s), 685 (m), 653 (m) (Fig.S1).

1.3 X-ray crystallographic study

All crystallographic data were collected on a Bruker APEX Ⅱ CCD diffractionmeter using Mo $K\alpha$ radiation (λ=0.071 073 nm) at 25 ℃. The structures were determined by direct methods and refined by the full-matrix least-squares method based on F^2 using SHELXL program and OLEX 2[24-25]. All nonhydrogen atoms were refined with anisotropic displacement parameters and hydrogen atoms were placed geometrically and refined using a riding model. Crystal structural parameters, some selected bond lengths and angles are listed in Table 1 and Table S1, respectively. The topology of CPs was analyzed by using TOPOs 4.0 program package[26].

CCDC: 1911100, **1**; 1911101, **2**.

Table 1　Crystal structure data and refinement parameters of 1 and 2

	1	2
Empirical formula	$C_{50}H_{40}N_8O_9Zn_2$	$C_{25}H_{21}N_4NiO_5$
Formula weight	1 027.64	516.17
Temperature / K	296.15	298(2)
Crystal system	Monoclinic	Triclinic
Space group	$P2_1$	$P\bar{1}$
a / nm	0.735 9(7)	0.907 7(3)
b / nm	1.901 7(18)	1.009 8(4)
c / nm	1.610 0(15)	1.717 9(6)
α / (°)		94.964(3)
β / (°)	94.683(11)	103.998(3)
γ / (°)		108.727(3)
Volume / nm^3	2.246(4)	1.423 7(9)
Z	2	2
D_c / ($g\cdot cm^{-3}$)	1.520	1.204
μ / mm^{-1}	1.137	0.718
F(000)	1 056.0	534.0
2θ range for data collection / (°)	5.078~49.998	4.944~55.426
Reflection collected	11 712	19 215
Independent reflection	4 988	6 581
R_{int}	0.092 8	0.053 1
Data, restraint, parameter	4 988, 1, 623	6 581, 0, 336
Goodness-of-fit on F^2	1.051	1.023
R_1, wR_2 [$I\geqslant 2\sigma(I)$]	0.061 9, 0.113 2	0.040 7, 0.093 0
R_1, wR_2 (all data)	0.110 3, 0.132 8	0.058 5, 0.099 4

2 Results and discussion

2.1 IR spectra

The absorption spectrum at 3 440~3 460 cm^{-1} corresponds to the characteristic peak of the stretching vibration of the O-H group in water molecules. The peaks at 1 393 cm^{-1} (**1**) or 1 376 cm^{-1} (**2**) and 1 630 cm^{-1} (**1**) or 1 546 cm^{-1} (**2**) are attributed to the symmetric and asymmetric stretching vibration of the carboxylate group, respectively. For **1**~**2**, the lack of strong peak in a range of 1 690~1 730 cm^{-1} demonstrates that the H_4tptc ligand is completely deprotonated

(Fig.S1).

2.2 Descriptions of crystal structures

2.2.1 Crystal structure of $\{[Zn_2(tptc)(1,4\text{-bimb})_2]\cdot H_2O\}_n$ (**1**)

Complex **1** crystallizes in the monoclinic system with the $P2_1$ space group. Its asymmetric unit contains two Zn^{2+} ions, one $tptc^{4-}$ linker, two 1,4-bimb linkers and one lattice water molecule. Both Zn^{2+} ions are four-coordinated and exhibit distorted tetrahedron geometries (Fig.1a). Each Zn^{2+} ion is bound to two oxygen atoms of two distinct $tptc^{4-}$ linkers and two nitrogen atoms provided by two 1,4-bimb ligands. The bond angles around Zn^{2+} range from 97.7° to 129.1°, and the bond lengths of Zn-O and Zn-N vary from 0.193 4 to 0.197 1 nm and 0.200 4 to 0.202 1 nm, respectively.

The H_4tptc ligands in **1** are completely deprotonated. All carboxylate groups adopt monodentate bridging coordination modes to link Zn^{2+} ions forming a 2D network (Fig.1b), which are further expanded by 1,4-bimb linkers to construct 3D structures (Fig.1c). Topologically, complex **1** reveals a 2-nodal (4,4)-c network with the topology of (8^6) by denoting Zn^{2+} ions and H_4tptc ligands to be 4-c nodes, respectively.

2.2.2 Crystal structure of $\{[Ni(tptc)_{0.5}(1,2\text{-bimb})(H_2O)]\cdot H_2O\}_n$ (**2**)

Complex **2** crystallizes in the triclinic system $P\bar{1}$ space group. There are one Ni^{2+} ion, half of $tptc^{4-}$ linkers, one 1,2-bimb, and one coordinated water molecule in the asymmetric unit of **2**. As exhibited in Fig.2a, each Ni^{2+} ion is coordinated by three carboxylate O atoms (Ni1-O1 0.214 26 nm, Ni1-O2 0.214 44 nm, Ni1-O3^{i} 0.202 80 nm), a lattice water O atom (Ni1-O5W 0.207 47 nm), and two N atoms of two 1,4-bimb (Ni1-N1 0.205 47 nm and Ni-N4^{ii} 0.206 35 nm), presenting a pseudo-octahedral geometry. The bond angles around Ni1 range from 61.46° to 179.23°.

As shown in Fig.2b, four carboxylate groups of

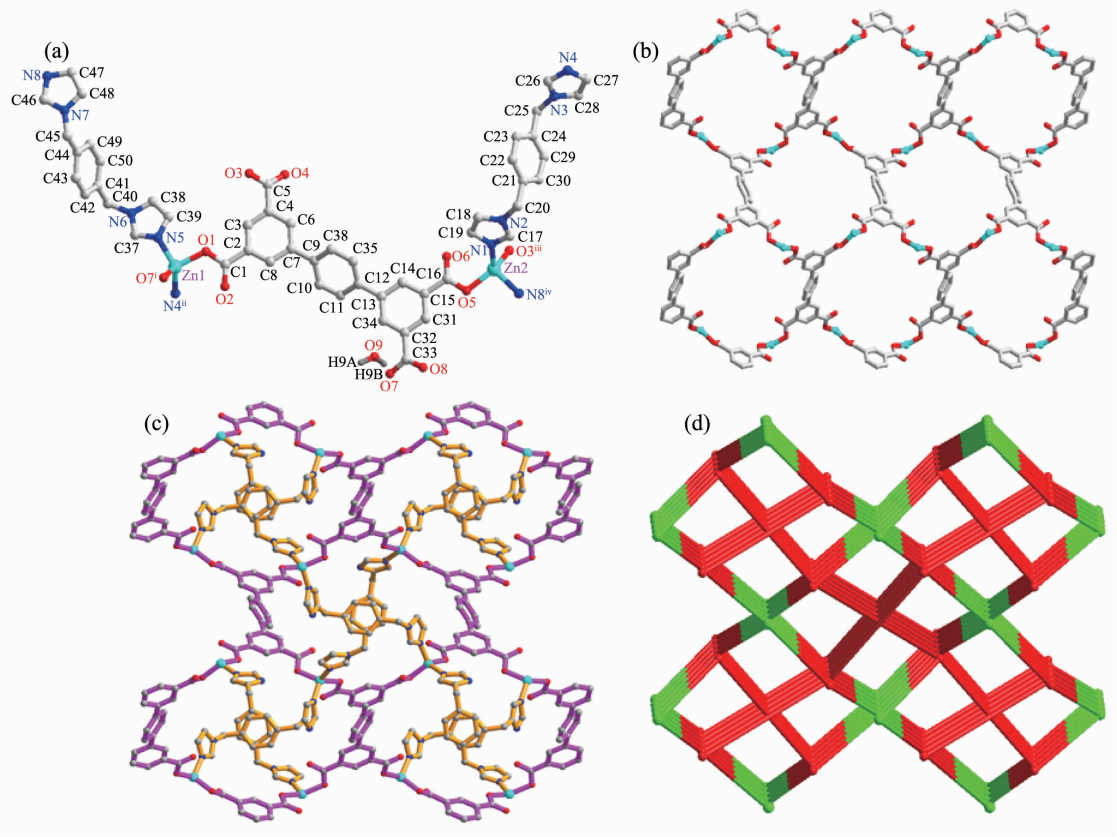

Symmetry codes: ^{i} 2−x, −0.5+y, 1−z; ^{ii} 3+x, y, 1+z; ^{iii} 1−x, 0.5+y, −z; ^{iv} −3+x, 1+y, z

Fig.1 (a) Coordination environment of Zn^{2+} ions in **1**; (b) 2D network of **1** based on Zn^{2+} ion and $tptc^{4-}$ observed along *a*-axis; (c) 3D structure of **1** viewed along *a*-axis; (d) Overall topological network for complex **1**

the H_4tcpb ligand adopt two different coordination patterns (bridging mode and chelating mode). The H_4tcpb ligands link the Ni^{2+} ions to get an interesting 1D rectangle chain (Fig.3a), while 1,2-bimb ligands link with the Ni^{2+} ions to form a 1D $[Ni(1,2\text{-bimb})]_n$ linear chain (Fig.3b). These two chains intertwine each other to form a 2D sheet by sharing metal centers (Fig.3c). Finally, 3D supramolecular structure is formed through O5W –H5WA ··· O2 and O5W – H5WB···O4 hydrogen bonds interactions between the adjacent sheets (Fig.4). Topological analysis indicates that the framework of **2** can be simplified to a new

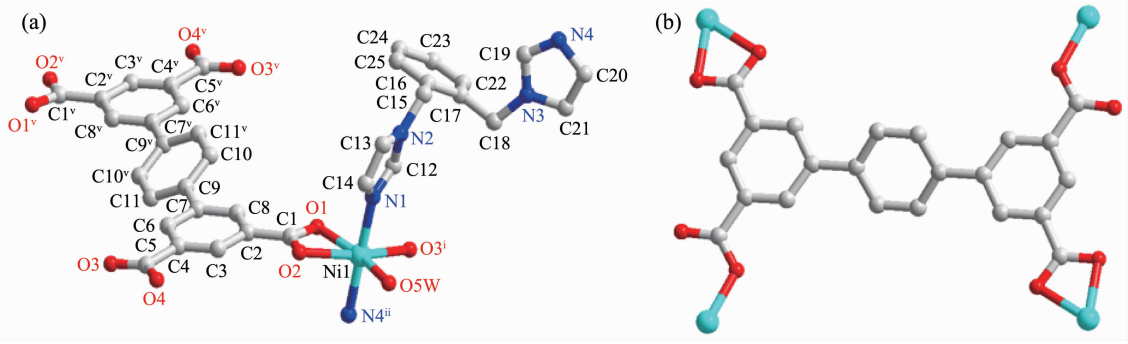

Symmetry codes: [i] $x, -1+y, z$; [ii] $1+x, 1+y, z$; [v] $1-x, 3-y, 2-z$

Fig.2　(a) Coordination environment of Ni^{2+} ions in **2**; (b) Coordination mode of the H_4tcpb ligand in complex **2**

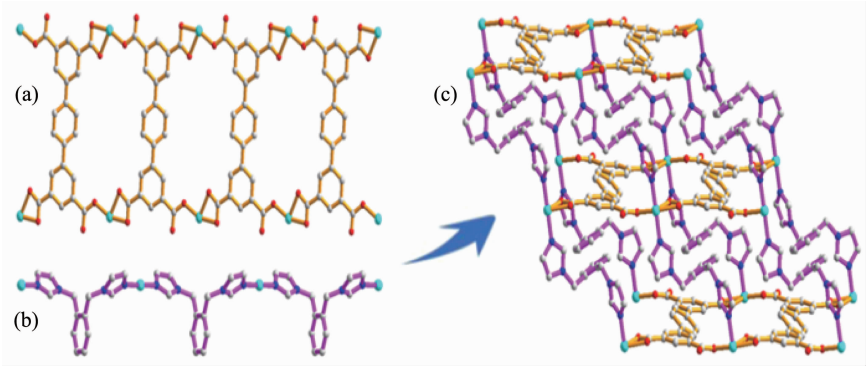

Fig.3　(a) One dimensional rectangle chain based on H_4tcpb and Ni^{2+} ions; (b) 1D $[Ni(1,2\text{-bimb})]_n$ linear chain constructed by 1,2-bimb ligands and Ni^{2+} ions; (c) View of the 2D network of **2**

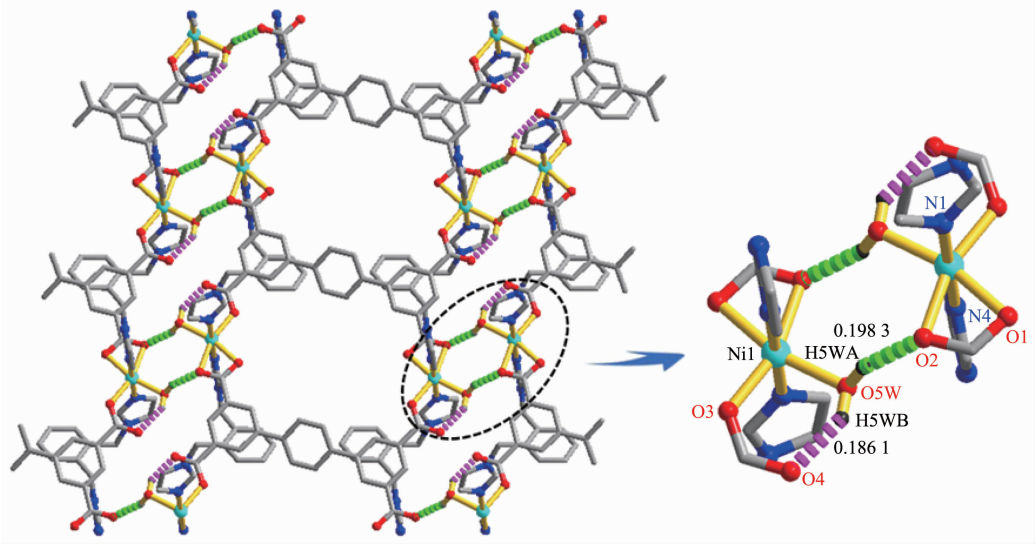

Hydrogen bonds are showed by dotted lines

Fig.4　Hydrogen bonds between adjacent 2D layers of **2**

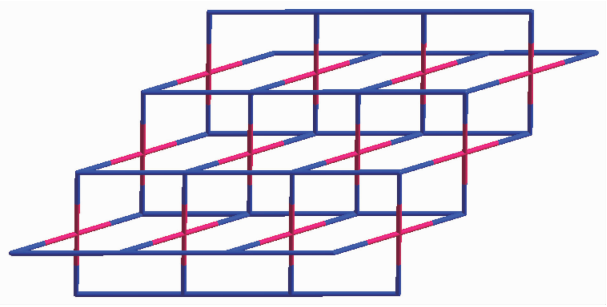

Fig.5 Schematic diagram of the 4,4-connected net of **2** with the point symbol of$\{4.6^4.8\}_2\{4^2.6^4\}$

(4,4)-c network with the point symbol of $\{4.6^4.8\}_2\{4^2.6^4\}$, where H_4tptc ligands and Ni^{2+} ions are taken as 4-connected nodes, respectively.

2.3 Powder X-ray diffraction analyses and TGA analyses

To evaluate the phase purity of CPs, the PXRD patterns of the as-synthesized samples were analyzed at ambient temperature (Fig.S2). The key peaks of the experimental PXRD patterns were almost consistent with the simulated ones, indicating that the phase purity of CPs is good. The difference in strength may be caused by the preferred orientation of crystal powder samples.

As shown in Fig.S3, complex **1** exhibits a weightlessness of 1.76% (Calcd. 1.75%) below 159 ℃, which is attributed to the loss of a lattice water molecule. After that, its framework is stable below 400 ℃. As for **2**, the first weight loss of 6.88% (Calcd. 6.74%) corresponds to the release of a lattice water and a coordinated water molecule under 196 ℃. The framework of **2** started to break down after 396 ℃.

2.4 Luminescence properties

The luminescence properties of ligands (H_4tptc and 1,4-bimb) and complex **1** were measured under room temperature (Fig.6). The emission spectra of H_4tptc and 1,4-bimb ligands were observed at 408 and 457 nm (λ_{ex}=280 nm), respectively, which can be attributed to the π-π* and π*-n transition[27-31]. Furthermore, compared with the emission bands of H_4tptc and 1,4-bimb, complex **1** was blue-shifted and exhibited an obvious emission maximum at 359 nm (λ_{ex}=280 nm). This is due to structural changes in ligands because of coordination with metal ions, which greatly enhances the rigidity of CP and decreases the energy loss through radiation less decay[32].

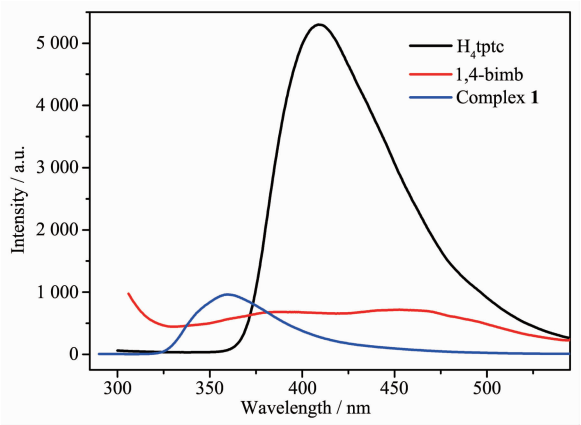

Fig.6 Solid-state luminescence emissions of H_4tptc, 1,4-bimb and complex **1**

In addition, from the perspective of practical application, the luminescence sensing properties of **1** in common solvents are also investigated. The ground samples were dispersed in different solvents (2 mL), including H_2O, DMA, DMF, methanol, acetonitrile, ethanol, acetone, DMSO, *etc*., by ultrasonic treatment for 30 min to obtain uniform **1**@solvent suspensions. As exhibited in Fig.7, the luminescence intensity of **1** depends on the types of the solvent. It is worth noting that **1** exhibited the strongest emission peak in H_2O and the weakest emission in acetone, which may be the result of interaction between the network of CPs and solvent molecules with disparate polarities[33].

Furthermore, because of water stability of

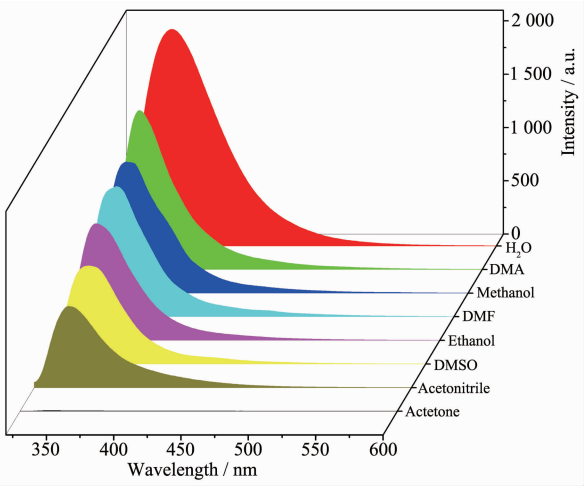

Fig.7 Luminescence intensities of complex **1** scattered in different organic solvents

complex **1**, luminescence sensing properties of **1** towards metal ions in aqueous solution were carried out. The finely ground sample of **1** was dispersed in $M(NO_3)_x$ aqueous solutions (0.01 mol·L^{-1}, M=Na$^+$, Cd^{2+}, K$^+$, Cu^{2+}, Pb^{2+}, Ag$^+$, Fe^{3+}, Mn^{2+}, Cr^{3+}, Zn^{2+}, Co^{2+}, Ni^{2+}, Ba^{2+}, Al^{3+}, Hg^{2+}, Ni^{2+}) to form **1**@M suspensions treated by the ultrasonic for 30 min. As presented in Fig.8, the luminescence intensity of **1** presents ion-dependent changes. Al^{3+} and Na$^+$ ions enhanced its luminescence intensity, while the other cations reduced its luminescence intensities. Particularly, the luminescence intensity of **1** was almost completely quenched by Fe^{3+} ion, implying that **1** can be one of the luminescent probes sensing Fe^{3+} ion.

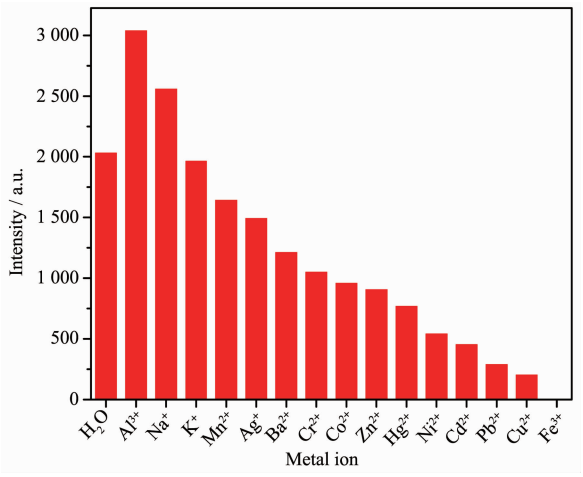

Fig.8　Luminescence intensity of complex **1** in different cationic water solutions

To test the sensitivity of **1** for sensing Fe^{3+} ion, the titration experiments were carried out. 2 mg crystal samples were dispersed in 3 mL aqueous solution to form **1**@H_2O suspensions, and then 30 μL $Fe(NO_3)_3$ solution (0.01 mol·L^{-1}) was gradually added into the above suspensions at a time. As can be seen in Fig.9, the luminescence intensity of **1**@H_2O suspension decreases gradually with the addition of Fe^{3+} ion. When the concentration of Fe^{3+} ion was 0.7 mmol·L^{-1}, the luminescence intensity of **1** was almost completely quenched. The relationship between I_0/I and the concentration of Fe^{3+} ion can be expressed by the equation of $I_0/I=0.74\exp(c_M/0.26)+0.44$, where c_M represents the concentration of Fe^{3+}, I_0 and I stand for luminescence intensities of **1**@H_2O and **1**@Fe^{3+} suspension, respectively. When the concentration of Fe^{3+} ion is low, the Stern-Volmer (S-V) curve can be expressed as a linear equation of $I_0/I=1+K_{sv}c_M$ (Fig.9)[34]. The K_{sv} value of Fe^{3+} was 5.29×10^3 L·mol^{-1}. The detection limit was calculated by $3\sigma/K_{sv}$ to be as low as 4.63×10^{-4}

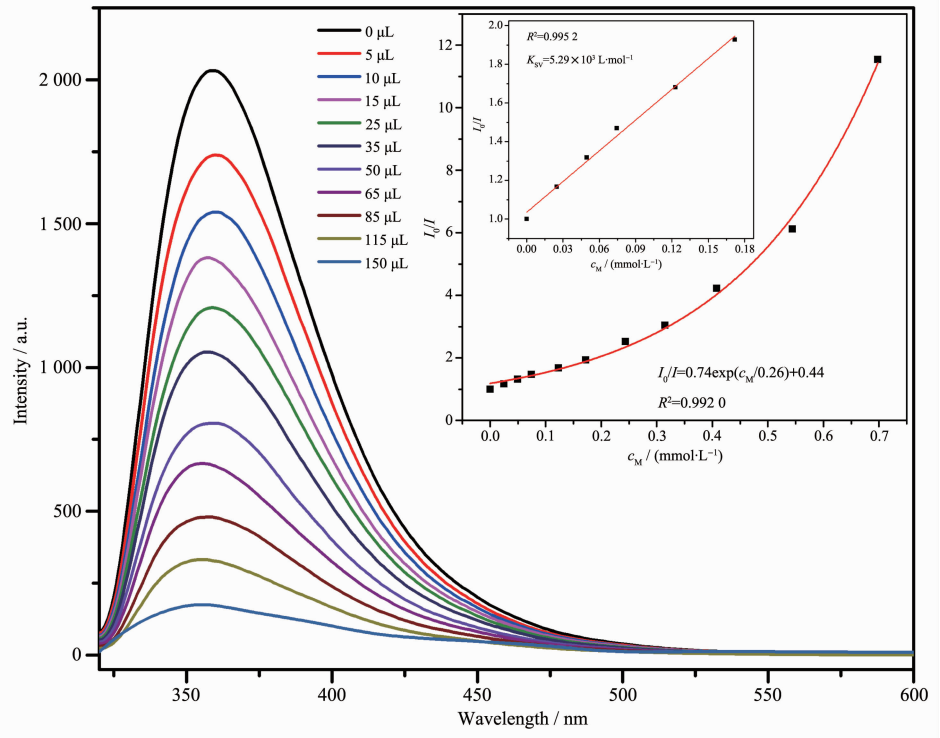

Fig.9　Influence of the addition of Fe^{3+} ions on the emission spectra of **1** dispersed in water solution

mol·L^{-1} (σ is the standard deviations by measuring the blank solution for 5 times at room temperature).

The luminescence experimental procedure of anions is similar to that of cations except substituting $M(NO_3)_x$ with K_nX (0.01 mol·L^{-1}, X=$Cr_2O_7^{2-}$, HPO_4^{2-}, SCN^-, CO_3^{2-}, $H_2PO_4^-$, I^-, HCO_3^-, PO_4^{3-}, Br^-, SCN^-, SO_4^{2-}, $H_2PO_4^-$ and Cl^-). As exhibited in Fig.10, compared to other anions, $Cr_2O_7^{2-}$ ion has the remarkable quenching effect to the luminescence of **1**. Similarly, the titration experiment of $Cr_2O_7^{2-}$ anion is shown in Fig.11, and the S-V curve is linear at low concentration and gradually deviated from linearity with the increasing of $Cr_2O_7^{2-}$ concentration. The quenching constant (K_{SV}) was calculated to be 6.15×10^3 L·mol^{-1}, which was higher than that of the reported MOFs for sensing $Cr_2O_7^{2-}$ ions (Table S2)[35-36].

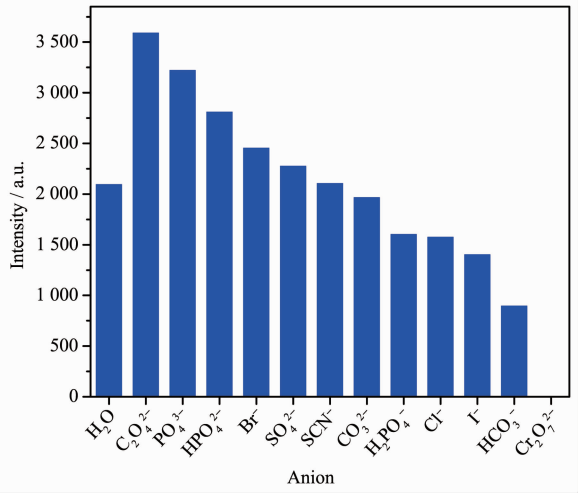

Fig.10 Luminescence intensity of complex **1** in aqueous solution containing different anions

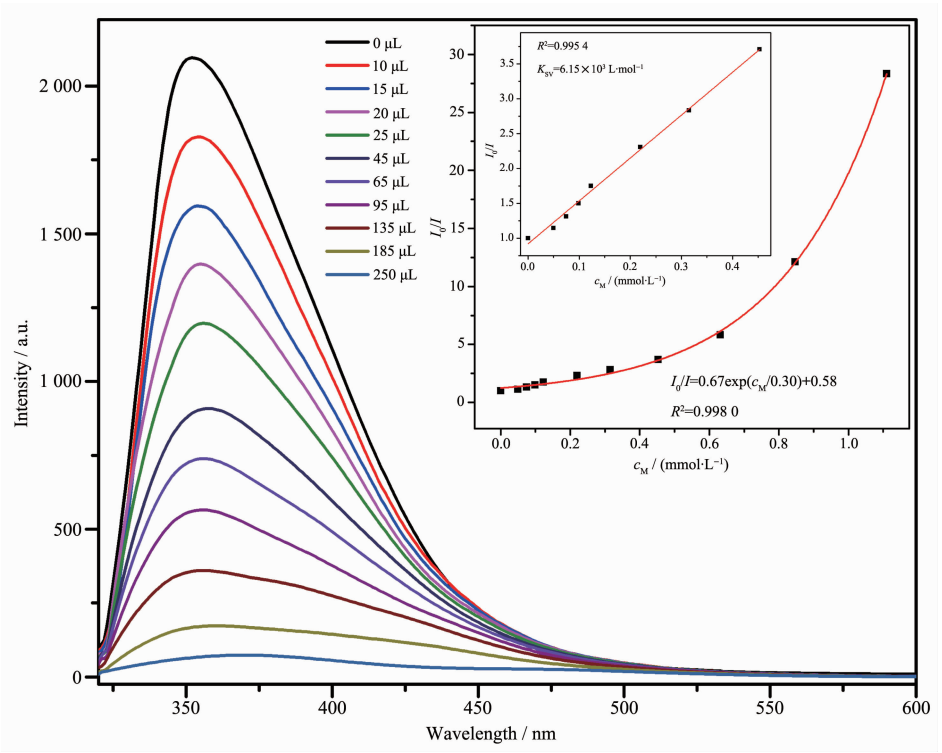

Fig.11 Influence of the addition of $Cr_2O_7^{2-}$ ions on the emission spectra of **1** dispersed in water solution

2.5 Quenching mechanism

In order to explore the mechanism of luminescence quenching, PXRD patterns of samples were measured before and after luminescence experiment, and the results showed that PXRD patterns of samples after luminescence experiment were almost identical with those of the original ones, which indicates that the structural collapse of complex is not the cause of luminescence quenching (Fig.S4). Furthermore, the UV-Vis absorption spectra (Fig.S5) showed that there were the partial overlap between the excitation band of **1** and the absorption band of $Fe^{3+}/Cr_2O_7^{2-}$ ions, which shows the competitive absorption of energy between the frameworks and that $Fe^{3+}/Cr_2O_7^{2-}$ ions is

responsible for luminescence quenching[37].

2.6 Magnetic properties

The direct-current (dc) magnetic susceptibility of **2** was measured in a temperature range of 2~300 K under a 1 000 Oe applied field. As exhibited in Fig. 12, the $\chi_M T$ value is 1.08 $cm^3 \cdot K \cdot mol^{-1}$ at room temperature, which is close to the theoretical value of 1.0 $cm^3 \cdot K \cdot mol^{-1}$ for one isolated Ni^{2+} ion (S=1, g=2.0). The $\chi_M T$ value decreased slowly to 0.49 $cm^3 \cdot K \cdot mol^{-1}$ at 30 K, and then decreased sharply, which may be attributed to the antiferromagnetic interaction between Ni^{2+} ions. Furthermore, the curve of the reciprocal susceptibilities (χ_M^{-1}) vs T was well fitted by the Curie-Weiss law: $\chi_M T = C/(T-\theta)$, which gave C=1.07 $cm^3 \cdot K \cdot mol^{-1}$ and θ=−2.68 K in a temperature range of 50~300 K, confirming the antiferromagnetic interaction between Ni^{2+} ions.

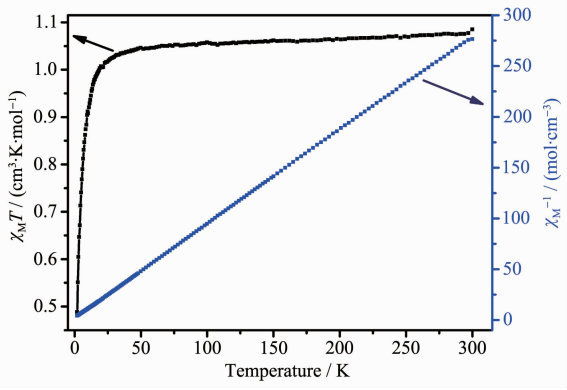

Fig.12　Temperature properties of $\chi_M T$ vs T and χ_M^{-1} vs T for **2**

3 Conclusions

In short, two new CPs have been successfully synthesized by utilizing the mixed ligands strategy. Complex **1** shows a 3D network with the point symbol of (8^6), and complex **2** is a 3D supramolecular architecture formed by the H-bond interaction between the adjacent 2D layers. Furthermore, the luminescence properties show that **1** has good sensing selectivity for Fe^{3+}/$Cr_2O_7^{2-}$ ions in aqueous solution, which indicates **1** has potential application in the detection of Fe^{3+} and $Cr_2O_7^{2-}$ ions. Moreover, magnetic measurements indicate that there is the antiferromagnetic interaction between Ni^{2+} ions in **2**.

Acknowle dgements: The authors sincerely thank the National Natural Science Foundation of China (Grant No. 21676258), the international Scientific and Technological Cooperation Projects of Shanxi Province (Grant No.201803D421080). Meanwhile, the authors honestly acknowledge the support of innovative investigated group of inorganic-organic mixed functional materials in North University of China.

Supporting information is available at http://www.wjhxxb.cn

References:

[1] Duan J, Jin W, Kitagawa S. *Coord Chem Rev.*, **2017**,**332**:48-74

[2] Zhang Y B, Zhang W X, Feng F Y, et al. *Angew. Chem. Int. Ed.*, **2009**,**48**(29):5287-5290

[3] Samaddar P, Son Y S, Tsang D C W, et al. *Coord. Chem. Rev.*, **2018**,**368**:93-114

[4] Zhang S F, Xiong F, He Z, et al. *Polyhedron.*, **2015**,**102**:401-409

[5] YANG Bing-Bing(杨冰冰), ZHAO Feng (赵丰), XU Sheng-Xian(许胜先), et al. *Chinese J. Inorg. Chem.*(无机化学学报), **2019**,**35**(6):1020-1026

[6] Xu L H, Fang G Z, Liu J F, et al. *J. Mater. Chem. A*, **2016**, **4**:15880-15887

[7] REN Li-Lei(任丽磊), PENG Xiao-Xia(彭晓霞), WANG Shu-Jun(王树军), et al. *Chinese J. Inorg. Chem.*(无机化学学报), **2019**,**35**(6):965-970

[8] Sun D, Liu F J, Huang R B, et al. *CrystEngComm*, **2012**,**14**: 7872-7876

[9] Luo X, Zhang X, Duan Y L, et al. *Dalton Trans.*, **2017**,**46** (19):6303-6311

[10]Cui P P, Zhao Y, Zhang X D, et al. *Dyes Pigm.*, **2016**,**124**: 241-248

[11]Zhang X T, Fan L M, Fan W L, et al. *Inorg. Chem. Acta*, **2016**,**441**:146-151

[12]Mukherjee S, Gole B, Song Y, et al. *Inorg Chem.*, **2011**,**50** (8):3621-3631

[13]Xie M H, Yang X L, Wu C D. *Chem. Commun.*, **2011**,**47** (19):5521-5523

[14]Manna K, Zhang T, Carboni M, et al. *J. Am. Chem. Soc.*, **2014**,**136**(38):13182-13185

[15]Lohar S, Banerjee A, Sahana A, et al. *Anal. Methods*, **2013**, **5**(2):442-445

[16]Sun X, Wang Y, Lei Y, et al. *Chem. Soc. Rev.*, **2015**,**44**(22): 8019-8061

[17]Zhou X, Lee S, Xu Z, et al. *Chem. Rev.*, **2015**,**115**(15):7944-8000

[18]Bobbitt N S, Mendonca M L, Howarth A J, et al. *Chem. Soc. Rev.*, **2017**,**46**:3357-3385

[19]Liu B B, Lin X L, Li H, et al. *Cryst. Growth Des.*, **2015**,**15**:4355-4362

[20]Hu F L, Shi Y X, Chen H H, et al. *Dalton Trans.*, **2015**,**44**(43):18795-18803

[21]Chen Z, Sun Y W, Zhang L L, et al. *Chem. Commun.*, **2013**, **49**:11557-11559

[22]Thompson C M, Kirman C R, Proctor D M, et al. *J. Appl. Toxicol.*, **2014**,**34**(5):525-536

[23]Wang C C, Li H Y, Guo G L, et al. *Transition Met. Chem.*, **2013**,**38**(3):275-282

[24]Sheldrick G M. *SADABS, Ver.*2.05, University of Göttingen, Germany, **1996**.

[25]Sheldrick G M. *SHELXS*-97, *Program for Crystal Structure Refinement*, University of Göttingen, Germany, **1997**.

[26]Sarkisov L, Martin R L, Haranczyk M, et al. *J. Am. Chem. Soc.*, **2014**,**136**(6):2228-2231

[27]Su Z, Fan J, Okamura T. *Cryst. Growth Des.*, **2010**,**10**(4):1911-1922

[28]Wudkewych M J, Laduca R L. *Polyhedron*, **2016**,**114**:72-79

[29]Yang X F, Zhu H B, Liu M. *Polyhedron*, **2017**,**128**:18-29

[30]Hong M M, Liu A F, Xu Y, et al. *Chin. Chem. Lett.*, **2016**, **27**:989-992

[31]SHA Qiu-Yue(沙秋月), YUAN Xue-Mei(袁雪梅), WANG Xiao-Yu(王小雨), et al. *Chinese J. Inorg. Chem.*(无机化学学报), **2016**,**32**(7):1293-1302

[32]Li Z H, Xue L P, Li S H. *CrystEngComm*, **2013**,**15**(14):2745-2754

[33]Zeng G, Xing S, Wang X, et al. *Inorg. Chem.*, **2016**,**55**(3):1089-1095

[34]Zhang X, Wang Z J, Chen S G, et al. *Dalton Trans.*, **2017**, **46**(7):2332-2338

[35]Cao C, Hu H C, Qiao W Z, et al. *CrystEngComm*, **2016**,**18**(23):4445-4451

[36]Parmar B, Rachuri Y, Bisht K K, et al. *Inorg. Chem.*, **2017**, **56**(5):2627-2638

[37]Wen R M, Han S D, Ren G J, et al. *Dalton Trans.*, **2015**,**44**(24):10914-10917